Journal of the Korean Ceramic Society
Vol. 45, No. 12, pp. 782~787, 2008.

Nanocomposite Ni-CGO Synthesized by the Citric Method as a Substrate for Thin-film IT-SOFC

Zhenwei Wang, Yu Liu*, Shin-ichi Hashimoto, and Masashi Mori†**

Central Research Institute of Electric Power Industry 2-6-1 Nagasaka, Yokosuka, Kanagawa 240-0196, Japan
**Shanghai Institute of Ceramics, Chinese Academy of Sciences 1295 Dingxi Road, Shanghai 200050, P. R. China*
***Tohoku University 6-6-11 Aoba, Aramaki, Aoba-ku, Sendai 980-8579, Japan*
(Received October 15, 2008; Revised December 22, 2008; Accepted December 22, 2008)

ABSTRACT

Ni-ceria cermets have been extensively investigated as candidates for the anode in intermediate-temperature solid oxide fuel cells. We have used the citric method to synthesize nanocomposite powders consisting of NiO (Ni metal content: 40~60% by volume) highly dispersed in $Ce_{0.9}Gd_{0.1}O_{1.95}$ (CGO). The microstructure characteristics and sintering behaviors of the nanocomposites were investigated. No impurity phases were observed and the shrinkage of these substrates matched well with that of a CGO electrolyte with a specific surface area of 11 m^2/g. Densification of the CGO electrolyte layer to <5 μm thickness was achieved by co-firing the laminated electrolyte with the porous NiO-CGO substrate at 1400°C for 6 h.

***Key words*: SOFC, Anode, NiO, Ceria, Citric method, Sintering characteristics**

1. Introduction

There has been growing interest in intermediate-temperature solid oxide fuel cells (IT-SOFCs) operating at 500~700°C from the viewpoint of a quick start and the use of metallic cell components. In this temperature range, cermets composed of Ni and ceria, such as $Ce_{1-x}Gd_xO_{2-\delta}$ and $Ce_{1-x}Sm_xO_{2-\delta}$, have been extensively investigated for use as the anode in IT-SOFCs.[1)]

Sintering of Ni particles in the cermet is known to be an anode degradation factor.[2,3)] As Ni particles cohere during cell operation, the number of three phase boundaries (TPBs), which are the electrode reaction sites, diminishes and the electric current paths are interrupted. Additionally, the reaction rate of hydrogen gas at the TPBs decreases exponentially with decreasing operating temperature. These effects may seriously damage the potential of the cermet as an anode for intermediate-temperature operation. It is therefore necessary to develop high-performance Ni-cermets with many TPBs.

Ni-cermet microstructures are closely related to the processes for the preparation of the starting powder. Thus, selection and optimization of the powder fabrication processes are important in order to have many TPBs at the anode/electrolyte interface region. Composite anodes based on a mixture of NiO and ceria are generally prepared by a mechanical mixing process, which simply mixes the separately prepared NiO and ceria powders together by ball milling. This method cannot produce a reliable uniform distribution of Ni particles in the Ni-ceria matrix.[4)] Numerous studies of Ni dispersion in ceria cermets have been reported.[5-8)] Although chemical vapor deposition (CVD) and physical vapor deposition (PVD) are effective methods for obtaining nanoparticles, high cost represents a major barrier to mass production. In contrast, the citric method is a cost-effective process for the synthesis of nanosized ceramic powders on a large scale.[9)]

In this work, we have applied the citric method for preparing anode powders consisting of NiO (Ni metal content: 40~60 vol%) highly dispersed in $Ce_{0.9}Gd_{0.1}O_{1.95}$ (CGO). The microstructure characteristics and sintering behaviors of the nanocomposites were investigated as substrates for IT-SOFCs, and densification of the CGO electrolyte layer was attempted by co-firing the laminated electrolyte with the porous NiO-CGO substrate.

2. Experimental

NiO-CGO powders (Ni metal content: 40~60% by volume) were synthesized by the citrate method using aqueous solutions of $Ce_2(CO_3)_3 \cdot 8H_2O$, $Gd_2(CO_3)_2 \cdot nH_2O$, and $xNiCO_3 \cdot yNi(OH)_2 \cdot zH_2O$ as precursors. The concentration of the precursor materials was confirmed by inductively coupled plasma (ICP) analysis. The carbonates were mixed in stoichiometric proportions, and citric acid ($HO_2CCH_2C(OH)(CO_2H)CH_2CO_2H$) was added to the solution in a molar proportion equivalent to the amount of metal cations. The appropriate amount of ethylene glycol ($C_2H_2(OH)_2$) was added and the solution was stirred for 3 h at temperatures of 60~100°C to form a homogeneous chelate between the

†Corresponding author : Masashi Mori
E-mail : masashi@criepi.denken.or.jp
Tel : +81-46-856-2121 Fax : +81-46-856-5571

metal cations and the citrate anions. The gel was then dried and fired at 800°C for 5 h to remove any remaining organic materials. In this paper, the chemical compositions of the samples are given as xNiO-CGO (i.e., the ratio Ni:CGO is x:100-x by volume after reduction).

The sample powders were pressed into pellets 20 mm in diameter and approximately 2 mm thick under a pressure of 23 MPa. The green body was then sintered at selected temperatures with a heating rate of 200°C/h in air. The holding time at the selected temperatures was varied from 0 to 10 h. The density of the sintered pellets was determined from the observed size and weight of the pellets. The relative density was derived theoretically from the experimental lattice parameters and unit formula. The theoretical densities of CGO, NiO and Ni used were 7.21 g/cm^2, 6.96 g/cm^2 and 8.90 g/cm^2, respectively.

The compositions of all the samples were confirmed by powder X-ray diffractometry (XRD) (18 kW, ultraX 18TTR2-300, Rigaku, Japan). The particle size of the powders was measured using a laser diffraction particle size analyzer (LA-920, Horiba, Japan) and the specific surface area was measured by the Brunauer-Emmett-Teller (BET) adsorption isotherm method using N_2 gas (Flow Sorb 2-2330, Shimadzu, Japan). The microstructure of the sintered samples was recorded by scanning electron microscopy (SEM) and energy dispersive X-ray (EDX) analysis (S-3500H, Hitachi, Japan).

A thin CGO electrolyte layer on the anode substrate was fabricated by the slurry coating and co-firing process.[10] The substrate was prepared by extruding 50NiO-CGO nanocomposite with binder and pore former into a tube 2.4 mm in diameter. The electrolyte slurry that contained the CGO powders and the organic ingredients was coated on the anode, and then the green samples were allowed to dry gradually at room temperature for 12 h. The bi-layers of the anode substrate and the coated CGO electrolyte layer were co-fired at 1400°C for 6 h. The rate of heating and cooling after the organic compounds were burnt out was 200°C/h.

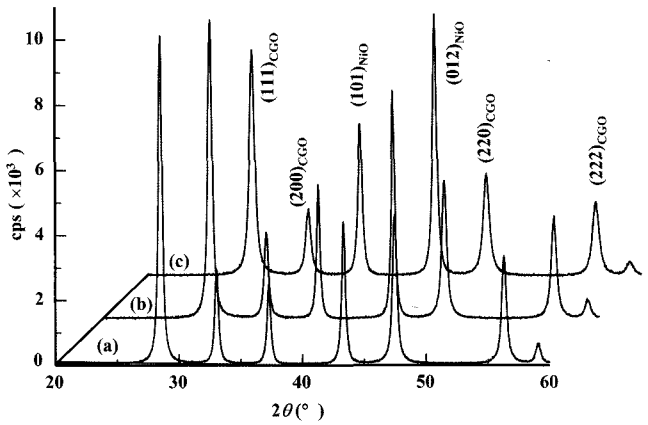

Fig. 1. XRD patterns of the NiO-CGO powders synthesized by the citric method after calcining at 800°C.

3. Results and Discussion

3.1. Phase characteristics of NiO-CGO synthesized by the citric method

Fig. 1 shows the XRD patterns (2θ=20–60°) of NiO-CGO sample powders after calcining at 800°C. It can be seen that the (012) reflection of NiO increases with increasing NiO content. All the peaks observed can be ascribed to the typical reflections from rhombohedral NiO (Space group R-3m, No.166)) and cubic CGO (Space group Fm3m, No.225). No peaks for impurities were observed. This suggests that the fluorite structure of CeO_2 and Gd_2O_3 is formed at the lower temperatures,[9] and a significant amount of NiO cannot diffuse into the fluorite oxide during powder preparation.

Fig. 2(a) shows the lattice parameter of CGO in the NiO-CGO powders before and after firing at 1400°C for 6 h. The lattice parameter of CGO after calcining at 800°C was almost the same as that reported previously.[11] It is interesting that a large difference appeared in the parameters between the samples fired at 800°C and 1400°C.

Fig. 2(b) shows the lattice parameters of NiO before and

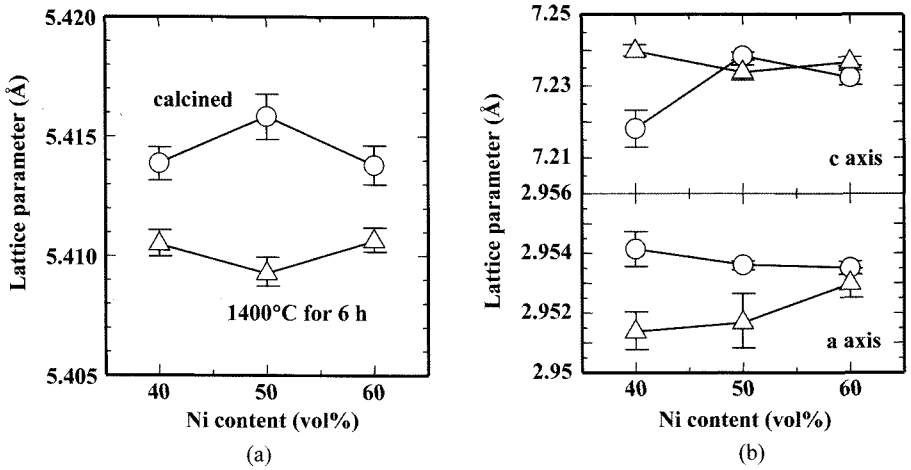

Fig. 2. Lattice parameters of the components in the NiO-CGO powders synthesized by the citric method: a) CGO and b) NiO. Circles and triangles represent the samples before and after firing, respectively.

Table 1. Lattice Parameters and Cell Volumes for CGO with Specific Surface Area of 11 m^2/g, NiO with Specific Surface Area of 4 m^2/g and 50NiO-CGO at Different Firing Stages

Samples	a (Å)	c (Å)	V ($Å^3$)	Remarks
CGO (raw material)	5.4173(6)	-	158.983	Base
CGO fired	5.4166(1)	-	158.924	Same
CGO in 50NiO-CGO fired	5.4145(2)	-	158.736	Decrease
NiO (raw material)	2.9546(3)	7.2385(6)	54.723	Base
NiO fired	2.9520(6)	7.237(1)	54.617	Decrease
NiO in 50NiO-CGO fired	2.9571(8)	7.225(4)	54.717	Same

after firing at 1400°C for 6 h. The lattice parameters, a and c, of NiO in the composites before and after firing become more similar with increasing NiO content.

In order to clarify the change in lattice parameters for nanosized NiO-CGO composites, pure CGO powders synthesized by the citric method were compared with those of the NiO-CGO composites. The specific surface area of CGO and NiO used were 11 m^2/g and 4 m^2/g, respectively. These materials are mixed into the 50NiO-CGO composite by the usual ceramic method. The lattice parameters are summarized in Table 1. After firing at 1400°C, the lattice parameter of the pure CGO did not change. However, an decrease in the lattice parameters of the CGO in 50NiO-CGO was observed after heat treatment. Thus, it is clear that the difference is related to the reaction between CGO and NiO. On the other hand, the lattice parameters of NiO decreased after firing, whereas for the mixture of NiO and CGO no significant change in the lattice parameters was observed.

It has been reported that lattice parameters can be changed by doping. For example, Gd-doping can increase lattice parameters: the lattice parameters of CeO_2 and $Ce_{0.9}Gd_{0.1}O_{1.95}$ are 5.4078 Å and 5.4217 Å, respectively.[12] Transition metal doping also increases lattice parameters.[13] The decrease in the lattice parameter for CGO in NiO-CGO can probably be explained by the diffusion of NiO into the cubic fluorite structure of CGO at relatively high temperatures, because the ionic radii are 83.0 pm for Ni^{2+}, 107.8 pm for Gd^{3+} and 101 pm for Ce^{4+}.[14] Also oxygen defect formation might contribute to the decrease in lattice parameters for pure NiO.[15] Therefore, the effect of the lattice parameters of NiO in the composites is greatest for low NiO content. On the other hand, no change in lattice parameters in NiO in NiO-CGO may be related to the diffusion of Ce and Gd elements and the oxygen defect formation during high-temperature heat treatment.

3.2. Morphological characteristics of the prepared powders

The citrate method can strongly inhibit grain growth and phase agglomeration for both NiO and CGO. Fig. 3 shows the SEM micrographs of the 50NiO-CGO powders after calcining at 800°C. The primary particles with an average size below 100 nm were highly aggregated. (Obviously it is difficult to distinguish the NiO grains from the CGO grains.) Transmission electron microscopy showed that the agglomeration of CGO particles synthesized by the citric method was very similar to the agglomeration of the CGO in the NiO-CGO mixtures.[9] The specific surface area and average particle size (D_{50}) are 15 m^2/g and 0.33 μm for 40NiO-CGO, 14 m^2/g and 0.40 μm for 50NiO-CGO, and 17 m^2/g and 0.26 μm for 60NiO-CGO. The particle size distributions of these powders are shown in Fig. 4. Two peaks were observed in the particle size distribution of the NiO-CGO powders, although the differences between the peaks were not statistically significant. The average size of the agglomeration of the fine CGO and NiO primary particles was approximately 500 nm.

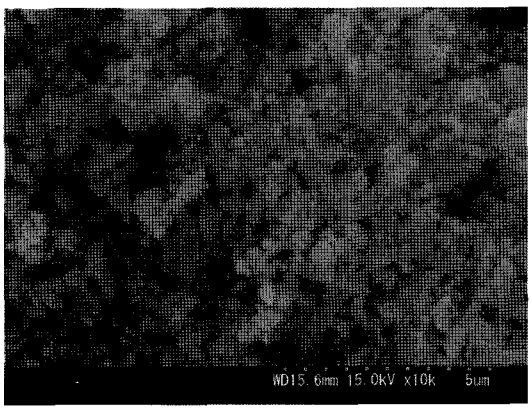

Fig. 3. SEM micrograph of the prepared 50NiO-CGO powder.

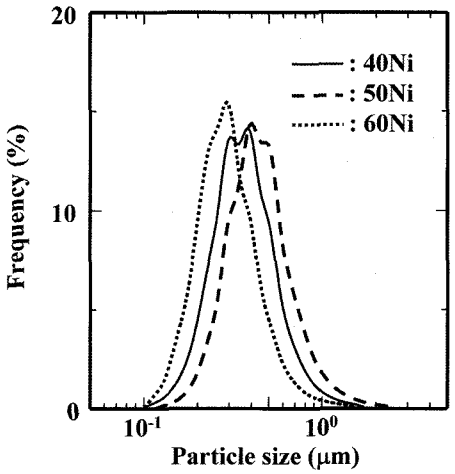

Fig. 4. Particle size distributions of the NiO-CGO powders synthesized by the citric method.

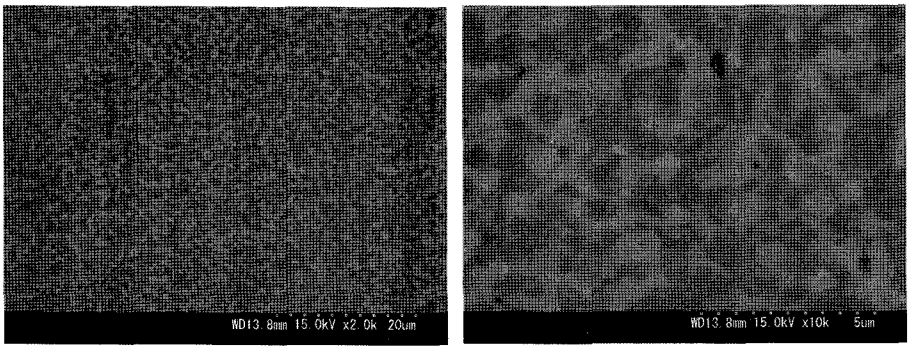

(a) (b)

Fig. 5. (a) BSE-SEM micrographs of 50NiO-CGO composite after firing at 1400°C for 10 h in air. Dark areas are NiO and the bright areas are CGO. (b) Enlargement of the area indicated in (a).

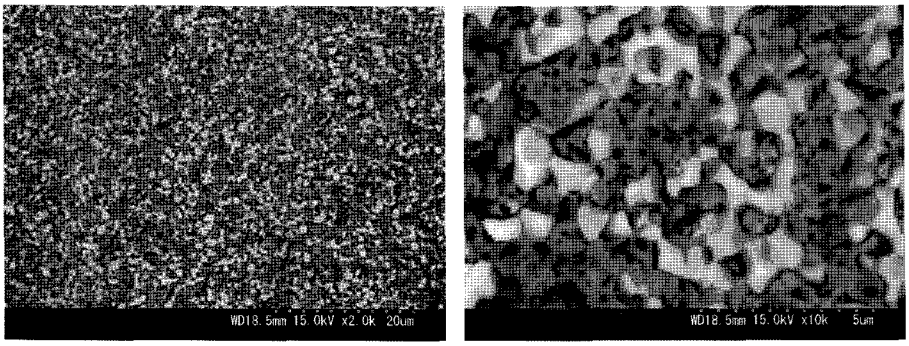

(a) (b)

Fig. 6. (a) BSE-SEM micrographs of 50Ni-CGO composite after firing at 1400°C for 10 h and further reducing at 600°C for 2 h in the H_2 atmosphere. White area is CGO and black part represents the pores formed by reducing NiO particles. Grayish areas between the white and black areas show Ni particles. (b) Enlargement of the area indicated in (a).

3.3. Microstructure of the sintered NiO-CGO samples

Fig. 5(a) and (b) show the Backscattered electron microscopy-SEM (BSE-SEM) micrograph of 50NiO-CGO sample after firing at 1400°C for 10 h in air. After sintering, the NiO and CGO adhered well. The NiO (dark areas) seemed to have an average size of 1 μm and to be homogeneously distributed throughout the CGO (bright areas). This maximizes the Ni/CGO/gas TPB in addition to maintaining electron paths through the anode.

Fig. 6(a) and (b) show the BSE-SEM micrographs of a 50Ni-CGO sample after firing at 1400°C for 10 h and further reducing at 600°C for 2 h in an H_2 atmosphere. The Ni-CGO composite has uniform, spherical pores (*ca.* 2~3 μm in diameter) and represents a well-bonded network. The high porosity of the composite and the good connection among the Ni-CGO grains not only enlarges the reactive areas, but also retains a high number of electron paths through the anode framework.

3.4. Sintering characteristics of NiO-CGO powders

Fig. 7(a) shows the relative density of the NiO-CGO powders to that of CGO with a specific surface area of 11 m^2/g and an average particle size of 0.17 μm. The samples with Ni contents of 40 vol% and 50 vol% had similar relative densities while the density of the 60NiO-CGO sample was lower. The CGO showed the highest sintering characteristics and the density reached ≥95% of the theoretical density at 1400°C for 6 h. The difference in sintering between NiO-CGO and CGO samples seems to prevent the diffusion of each component in the composites.

Densification of a thin electrolyte in the well-known wet-ceramic co-firing technique is generally achieved by co-sintering the laminate electrolyte with the support electrode at a relatively high temperature. Fig. 7(b) shows the shrinkage of the NiO-CGO powders synthesized by the citric method, compared with the CGO electrolyte. The shrinkage of the anode is well matched with that of the electrolyte in the temperature range 800~1400°C. The combination of CGO and NiO-CGO is appropriate for the co-firing fabrication of an anode supported thin-film cell.

3.5. Fabrication of an anode-supported thin-film CGO

A thin-film CGO electrolyte was fabricated on an NiO-CGO anode prepared by the citric method. Fig. 8(a) and (b)

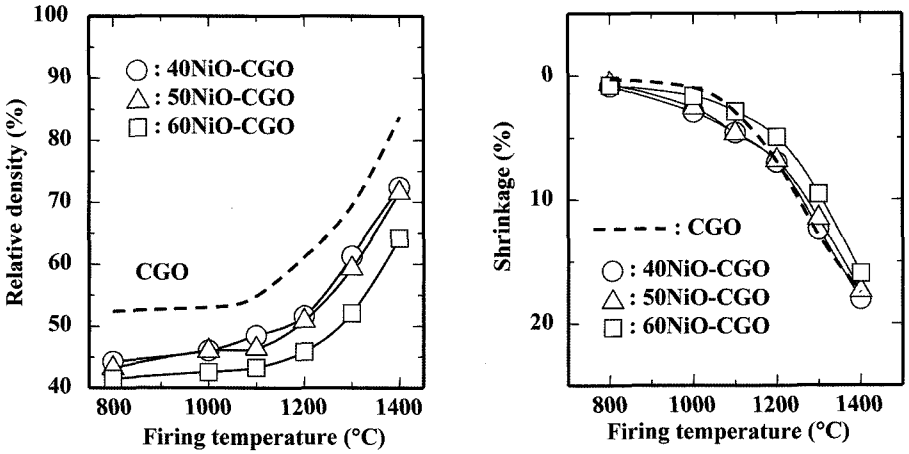

Fig. 7. Sintering characteristics of NiO-CGO powders synthesized by the citric method: (a) Relative density and (b) Shrinkage.

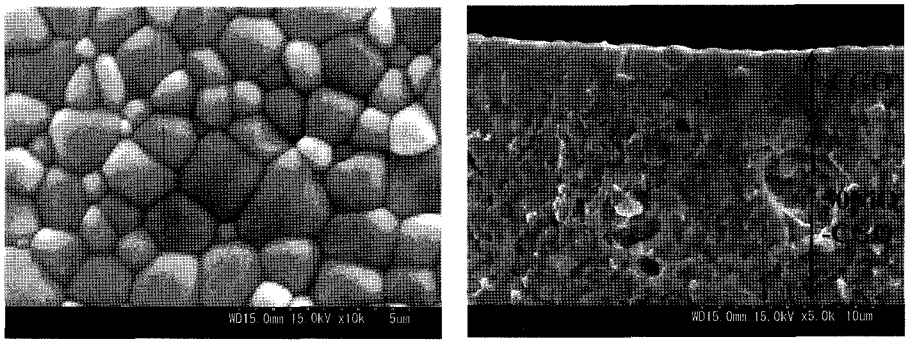

Fig. 8. SEM micrographs of microstructures of the CGO thin-film on a 50NiO-CGO anode substrate: (a) Surface section and (b) Cross section.

show the SEM micrographs of the surface and cross sections of the CGO thin-film on a supporting NiO-CGO anode after sintering at 1400°C for 6 h. The grain size was approximately 1~4 μm. The thickness of the CGO film was approximately ≤5 μm. No cracks or pinholes in the dense CGO were observed. Details of the microstructure and electrochemical behavior of the fabricated anode-supported cell will be reported elsewhere.

4. Conclusion

Nanocomposite powders consisting of NiO (Ni: 40~60 vol%) highly dispersed in $Ce_{0.9}Gd_{0.1}O_{1.95}$ (CGO) were synthesized by the citric method. The citric method strongly inhibits grain growth and phase agglomeration for both NiO and CGO. Sintering investigation suggests that the NiO-CGO nanocomposites are suitable substrates fore anode-supported IT-SOFCs made by co-firing with the electrolyte. A dense CGO electrolyte ≤5 μm thick has been successfully fabricated on a porous NiO-CGO substrate by a cost-effective technique involving slurry coating through co-firing at 1400°C for 6 h.

Acknowledgments

This work was supported by NEDO, Japan, as part of the Advanced Ceramic Reactor Project.

REFERENCES

1. W. Z. Zhu and S. C. Deevi, "A Review on the Status of Anode Materials for Solid Oxide Fuel Cells," *Material Science and Engineering*, **A362** 228-39 (2003).
2. H. Itoh, T. Yamamoto, M. Mori, T. Watanabe, and T. Abe, "Improved Microstructure of Ni-YSZ Cermet Anode for SOFC with a Long Term Stability," *Denki Kagaku*, **64** [6] 549-54 (1996).
3. H. Itoh, T. Yamamoto, M. Mori, T. Horita, N. Sakai, H. Yokokawa, and M. Dokiya, "Configurational and Electrical Behavior of Ni-YSZ Cermet with Novel Microstructure for Solid Oxide Fuel Cell Anodes," *J. Electrochem. Soc.*, **144** [2] 641-46 (1997).
4. Y. Liu, S. Hashimoto, K. Takei, M. Mori, and Y. Fanahashi,

"Development and Characterization of Cathode-supported SOFCs by Single-Step Cofiring Fabrication for Intermediate Temperature Operation," *J. Fuel Cell Sci. and Tech.*, [5] 031209-5 (2008).

5. T. Ishihara, T. Shibayama, H. Nishiguchi, and Y. Takita, "Nickel-Gd-doped CeO_2 Cermet Anode for Intermediate-temperature Operating Solid Oxide Fuel Cells using $LaGaO_3$-based Perovskite Electrolyte," *Solid State Ionics*, **132** 209-16 (2000).
6. S. Suzuki, H. Uchida, and M. Watanabe, "Microstructural Analyses of Ceria-Based Anode with Highly Dispersed Ni Electrocatalysts for Medium-Temperature Solid Oxide Fuel Cells," *Electrochem.*, **73** [2] 128-34 (2005).
7. T. Misono, K. Murata, J. Yin, and J. Fukui, "Morphology Control of Ni-GDC Cermet Anode for Lower Temperature," pp.1355-62 *in Proceedings of Solid Oxide Fuel Cells 10.* Eds. K. Eguchi, S. C. Singhal, H. Yokokawa, and J. Mizusaki, ECS Transactions Vol. 7 No.1 ISBN 978-1-56677-554-0 (2007).
8. S. Awatsu, H. Iwasaki, K. Isono, N. Chitose, G. Uozumi, T. Inagaki, and T. Ishihara, "Nano-metal Dispersed Anode of Intermediate-temperature SOFC for High Power Density Operation," pp.1583-1590 *in Proceedings of Solid Oxide Fuel Cells 10.* Eds. K. Eguchi, S. C. Singhal, H. Yokokawa, and J. Mizusaki, ECS Transactions Vol. 7 No.1 ISBN 978-1-56677-554-0 (2007).
9. M. Mori, E. Suda, and Y. Fujie, "Nano Cerium Oxide Powders as Electrolytes in Intermediate-temperature Solid Oxide Fuel Cells," *Recent Research Development: Solid State Ionics*, Transworld Research Network ISBN 81-7895-194-0 3 51-90 (2006).
10. Y. Liu, S. Hashimoto, H. Nishino, K. Takei, M. Mori, T. Suzuki, and Y. Fanahashi, "Fabrication and Characterization of Micro-tubular Cathode-supported SOFC for Intermediate Temperature Operation," *J. Power Sources*, **174** 95-102 (2007).
11. H. Inaba and H. Tagawa, "Ceria-based Solid Electrolyte," *Solid State Ionics*, **83** 1-16 (1996).
12. E. Suda, B. Pacaud, Y. Montardi, M. Mori, and Y. Takeda, "Electrical and Thermal Properties of Dense $Ce_{1-x}RE_xO_{2-\delta}$ Electrolyte using Low-temperature Sinterable Powder ($0 \leq x \leq 0.2$, RE=Y, Sm, Gd)," *Transactions of the Materials Research Society of Japan*, **29** [5] 2317-20 (2004).
13. M. Mori, E. Suda, B. Pacaud K. Murai, and T. Moriga, "Effect of Components in Electrodes on Sintering Characteristics of $Ce_{0.9}Gd_{0.1}O_{1.95}$ Electrolyte in Intermediate-temperature Solid Oxide Fuel Cells During Fabrication," *J. Power Sources*, **157** 688-94 (2006).
14. R. D. Shannon and C. T. Prewitt, "Effective Ionic Radii in Oxides and Fluorides," *Acta Crystalloger.*, **B25** 925-46 (1969).
15. K. Kosugi, "Non-stoichiometric Compounds," Baifukan, Tokyo ISBN4-563-04183-1 (1985).